

SMOOTH ADAPTIVE FINITE TIME ATTITUDE TRACKING CONTROL OF RIGID SPACECRAFT

HAITAO CHEN, XUEHUI LI AND SHENMIN SONG*

Center for Control Theory and Guidance Technology
Harbin Institute of Technology
No. 92, West Dazhi Street, Harbin 150001, P. R. China
cht2016hit@163.com; lxh_hit@126.com; *Corresponding author: songshenmin@hit.edu.cn

Received September 2016; revised February 2017

ABSTRACT. *This paper investigates two chattering-free finite-time controllers for the rigid spacecraft attitude tracking control problem considering modeling uncertainty and external disturbance. First, the basic controller is designed utilizing integral terminal sliding mode surface (ITSMS) with prior knowledge of the total system uncertainty consisting of modeling uncertainty and external disturbance. Second, an adaptive controller is proposed to deal with unknown system uncertainty through on line approximating upper bound information of the first derivative of the total system uncertainty. Compared with the existing literature, advantages of the proposed control laws include not only finite-time convergence rate for the closed-loop system robustness against uncertainty, but also chattering-free control signal since the derivative of the control input signal is designed directly and then the switch functions are hidden behind the integration operation. At last, rigorous stability proof is given via Lyapunov stability theory and digital simulations are undertaken to verify the effectiveness of the proposed controllers.*

Keywords: Attitude tracking control, Finite-time convergence, Chattering-free, Integral terminal sliding mode surface, Adaptive control

1. Introduction. Attitude tracking control of rigid spacecraft has attracted much attention due to its importance in many space missions. Many scholars have devoted to related researches and put forward various control methods considering the attitude tracking control problem, such as optimal control [1], nonlinear PD + control [2], back-stepping control [3], adaptive control [4] and variable structure control [5]. To satisfy the high demand of the advanced space missions, fast response, high control precision and robustness against many kinds of disturbances must be assured for the closed-loop spacecraft system. Therefore, the sliding mode control (SMC) methods [6,7] are favored, due to its strong robustness and easy interaction with other control procedures. Especially for the terminal sliding mode control (TSMC) [8], since its sliding mode surface contains a fractional power term and finite-time convergence for the system can be obtained, which gives the TSMC method great advantage in both practical and theoretical situations. Hence this paper utilizes the terminal sliding mode control method to solve the attitude tracking control problem.

The TSMC based finite-time control methods have been widely researched during the past decades. In [9], a modified nonsingular terminal sliding mode surface (NTSMS) based on [8] is firstly constructed for controlling the Euler-Lagrange system. In [10], a fast terminal sliding mode surface (FTSMS) based control law is proposed by adding a linear part to the conventional terminal sliding mode surface (TSMS) in [8]. [11] builds up a switching mechanism between conventional FTSMS and linear sliding mode surface (LSMS) around the origin to avoid the input singularity and speed up the convergence

rate. A fast nonsingular terminal sliding mode surface (FN-TSMS) based control method is then derived. Related result has been extended to the spacecraft attitude tracking control area in [12]. Recently, [13] utilizes the full-order sliding mode surface to formulate the controller for general systems, which not only eliminates the input singularity, but also achieves finite-time convergence. However, most of the above mentioned works, including [13], still depend on priori knowledge of the system uncertainty which may not be available in most practical situations. And by assigning high gains to respective switching controllers to suppress the system uncertainty and satisfy the stability theory, the control performance of these works can be highly affected. Therefore, further research is still necessary for the attitude tracking control problem with unknown system uncertainties.

Various methods can be associated with the TSMC methods to deal with unknown system uncertainty including adaptive control, neural networks and the observers. In [14], adaptive control method is used to estimate the upper bound of the system uncertainty, but the input singularity problem is neglected. In [15,16], the system uncertainty is compensated by neural networks. However, by adding switching function into the controllers or adaptive laws in [14-16], the controllers become discontinuous and the introduced input chattering can debase the system performance seriously if not being treated properly. Researchers have proposed different procedures to offset the input chattering problem. For instance, in [17,18], the second-order disturbance observer is utilized to estimate and compensate unknown system uncertainty online and at the same time attenuate the input chattering by lowering the controller gains, but upper bound of the second derivative of the system uncertainty is still needed. Fast-TSM-type reaching law is used to assure the steady states ultimately bounded and formulate continuous controllers in [18], but only uncertainties bounded by a constant can be handled by this method.

Given the previous analysis, it can be seen that, few of the existing studies can achieve robustness against unknown system uncertainty, fast finitetime convergence rate and chattering-free control input at the same time. Therefore, this paper proposes two chattering-free finite-time attitude tracking control laws considering the previous problems based on integral terminal sliding mode control and adaptive control laws. The main contributions of this paper are as follows. Compared with [9,10,12,13,17,18], both the proposed controllers are capable of dealing with system uncertainty and by utilizing the adaptive technique, the second controller can also deal with unknown system uncertainty; Compared with [11,14-16], input discontinuousness is avoided and the resultant controllers can be totally chattering-free.

The rest of the paper is organized as follows. In Section 2, preliminaries and system dynamics are established. Section 3 presents two robust chattering-free controllers and respective rigorous stability proofs. In Section 4, numerical simulations are undertaken. The paper is closed with some concluding remarks in Section 5.

2. Preliminaries.

2.1. Spacecraft attitude dynamics based on quaternion. The quaternion of the spacecraft body frame with respect to the inertial frame is denoted as $q = [q_0 \ q_v^T]^T = [q_0 \ q_1 \ q_2 \ q_3]^T$. The scalar part q_0 and the vector part q_v are subject to the constraint $q_0^2 + q_v^T q_v = 1$. $\omega \in R^{3 \times 1}$ denotes the angular velocity of the spacecraft in the body frame. $J \in R^{3 \times 3}$ is the inertia matrix of the spacecraft. $u \in R^{3 \times 1}$ and $d \in R^{3 \times 1}$ are the control torque and external disturbance torque. I_3 represents the 3×3 identity matrix. For any $a = [a_1, a_2, a_3]^T \in R^{3 \times 1}$, a^\times denotes the skew-symmetric matrix generated by a . Denote $q_d = [q_{d0} \ q_{dv}^T]^T$ as the desired attitude of the spacecraft in the reference frame, q_d^* as the conjugate quaternion of q_d and $\omega_d \in R^{3 \times 1}$ as the desired angular velocity resolved in

the reference frame. Define \tilde{q} and $\tilde{\omega}$ to represent the error quaternion and error angular velocity of the spacecraft which are calculated as $\tilde{q} = q_d^* \circ q = [\tilde{q}_0 \ \tilde{q}_v^T]^T = [\tilde{q}_0 \ \tilde{q}_1 \ \tilde{q}_2 \ \tilde{q}_3]^T$ and $\tilde{\omega} = \omega - C(\tilde{q})\omega_d$ where “ \circ ” is the multiplication operator between quaternion and $C = C(\tilde{q})$ is the rotation matrix from the reference frame to the spacecraft body frame defined as $C(\tilde{q}) = (\tilde{q}_0^2 - \tilde{q}_v^T \tilde{q}_v) I_3 + 2\tilde{q}_v \tilde{q}_v^T - 2\tilde{q}_0 \tilde{q}_v^\times$. Then it yields the error dynamic equations of the attitude tracking control system

$$\dot{\tilde{q}} = \frac{1}{2} \begin{bmatrix} -\tilde{q}_v^T \\ \tilde{q}_0 I_3 + \tilde{q}_v^\times \end{bmatrix} \tilde{\omega} \quad (1)$$

$$J\dot{\tilde{\omega}} = -(\tilde{\omega} + C(\tilde{q})\omega_d)^\times J(\tilde{\omega} + C(\tilde{q})\omega_d) + J(\tilde{\omega}^\times C(\tilde{q})\omega_d - C(\tilde{q})\dot{\omega}_d) + u + d \quad (2)$$

Assume that the inertia matrix in (2) is in the form of $J = J_0 + \Delta J$, where J_0 is the known positive constant matrix and ΔJ is the unknown inertia perturbation. Then it has

$$J_0 \dot{\tilde{\omega}} = F + u + \delta \quad (3)$$

where

$$F = -(\tilde{\omega} + C\omega_d)^\times J_0(\tilde{\omega} + C\omega_d) + J_0(\tilde{\omega}^\times C\omega_d - C\dot{\omega}_d) \quad (4)$$

$$\delta = [\delta_1 \ \delta_2 \ \delta_3]^T = \Delta F + d \quad (5)$$

$$\Delta F = -(\tilde{\omega} + C\omega_d)^\times \Delta J(\tilde{\omega} + C\omega_d) + \Delta J(\tilde{\omega}^\times C\omega_d - C\dot{\omega}_d) - \Delta J\dot{\tilde{\omega}} \quad (6)$$

δ is the total system uncertainty.

This paper aims at solving the rigid spacecraft attitude tracking control problem considering modeling uncertainty, external disturbance, input singularity and actuator chattering, which is equivalent to designing a chattering-free control input u for systems (1) and (2), so that finite time convergence of the attitude tracking error \tilde{q} and angular velocity tracking error $\tilde{\omega}$ is obtained even in the presence of modeling uncertainty and external disturbance.

3. Main Results. In this section, two robust chattering-free finite-time controllers are designed to deal with the problem of attitude tracking for rigid spacecraft considering modeling uncertainty and external disturbance. The fast nonsingular terminal sliding mode surface (FNTSMS), the integral terminal sliding mode surface (ITSMS) and some useful lemmas are introduced firstly.

The basic FNTSMS is firstly designed as:

$$S = [S_1 \ S_2 \ S_3]^T = \tilde{\omega} + \alpha_1 \tilde{q}_v + \alpha_2 \beta(\tilde{q}_v) \quad (7)$$

where

$$\beta(\tilde{q}_v) = [\beta(\tilde{q}_1) \ \beta(\tilde{q}_2) \ \beta(\tilde{q}_3)]^T \quad (8)$$

$$\beta(\tilde{q}_i) = \begin{cases} \text{sig}^\gamma(\tilde{q}_i) & |\tilde{q}_i| > \eta \\ r_1 \tilde{q}_i + r_2 \text{sgn}(\tilde{q}_i) \tilde{q}_i^2 & |\tilde{q}_i| \leq \eta \end{cases}, \quad i = 1, 2, 3 \quad (9)$$

$$r_1 = (2 - \gamma)\eta^{\gamma-1}, \quad r_2 = (\gamma - 1)\eta^{\gamma-2}, \quad 0 < \gamma, \eta < 1 \quad (10)$$

$$\text{sig}^\gamma(\tilde{q}_i) = \text{sgn}(\tilde{q}_i) |\tilde{q}_i|^\gamma, \quad i = 1, 2, 3 \quad (11)$$

$$\text{sgn}(\tilde{q}_i) = \begin{cases} 1 & \tilde{q}_i > 0 \\ 0 & \tilde{q}_i = 0 \\ -1 & \tilde{q}_i < 0 \end{cases}, \quad i = 1, 2, 3 \quad (12)$$

Motivated by [13], in order to provide chattering-free and finite-time stabilizing control input, the ITSMS $\sigma = [\sigma_1 \ \sigma_2 \ \sigma_3]^T$ is constructed as

$$\sigma = \dot{S} + k_1 S + k_2 \beta(S) \quad (13)$$

where S is defined in (7), $0 < \gamma_1 < 1$, k_1 and k_2 are positive constants, $\beta(\cdot)$ is similar to (8) and (9) except that respective parameters are set as γ_1 and η_1 which are all positive. Then it yields

$$\sigma = J_0^{-1}F + J_0^{-1}u + J_0^{-1}\delta + \alpha_1\dot{\tilde{q}}_v + \alpha_2\dot{\beta}(\tilde{q}_v) + k_1S + k_2\beta(S) \tag{14}$$

Lemma 3.1. [20] *For any real numbers n_i , $i = 1, \dots, n$ and $0 < c < 2$, the following inequality holds*

$$(n_1^2 + n_2^2 + \dots + n_n^2)^c \leq (n_1^c + n_2^c + \dots + n_n^c)^2 \tag{15}$$

Lemma 3.2. [12] *For system $y = f(x)$, $x \in R^{n \times 1}$, $f(0) = 0$. Assume $V(x)$ is C^1 smooth, positive definite and defined on $U \subset R^{n \times 1}$ and $\dot{V}(x) + aV(x)^c$ is negative semi-definite and defined on $U \subset R^{n \times 1}$, where $a > 0$, $0 < c < 1$, then there exists an area $U_0 \subset R^{n \times 1}$ such that any $V(x)$ starting from $U_0 \subset R^{n \times 1}$ is able to reach $V(x) \equiv 0$ in finite time. Moreover, if T is the time for $V(x) \equiv 0$ to be reached, then*

$$T \leq \frac{V(x(t_0))^{1-c}}{a(1-c)} \tag{16}$$

where $V(x(t_0))$ is the initial value of $V(x)$. And the system $y = f(x)$ is finite time stable.

Lemma 3.3. [20] *For system $y = f(x)$, $x \in R^{n \times 1}$, $f(0) = 0$. If $V(x)$ defined in Lemma 3.2 satisfies $\dot{V}(x) \leq -aV(x) - bV(x)^c$, where $a > 0$, $b > 0$, $0 < c < 1$. Then $V(x) \equiv 0$ can be reached after*

$$T \leq \frac{1}{a(1-c)} \ln \frac{aV(x(t_0))^{1-c} + b}{b} \tag{17}$$

3.1. Basic integral terminal sliding mode controller design. To facilitate the control system design in this subsection, the following assumption is introduced firstly.

Assumption 3.1. [13,19,21-23] *The total system uncertainty δ is upper bounded and its derivative $\dot{\delta}$ is also upper bounded as $\|\dot{\delta}\|_1 < l$, where $\|\dot{\delta}\|_1$ represents the 1-norm of $\dot{\delta}$ and l is a positive constant.*

Remark 3.1. *The total uncertainty δ contains both external disturbance and modeling uncertainty. Assumption 3.1 means that both the total uncertainty and its first derivative are upper bounded, which agrees with most of the practical situations. For example, when the spacecraft system or other plants are under control, the control torques may vary with the system states, but the change rate of the control torques and system states cannot be infinite in practical situations, which is shared by many works [13,19,21-23].*

Based on previous analysis, the following controller is proposed:

$$u = -F - \alpha_1 J_0 \dot{\tilde{q}}_v - \alpha_2 J_0 \dot{\beta}(\tilde{q}_v) - k_1 J_0 S - k_2 J_0 \beta(S) - \int_0^t l \operatorname{sgn}(\sigma) d\tau \tag{18}$$

where l is defined in Assumption 3.1.

Then it yields the following theorem.

Theorem 3.1. *Consider the system described by (1) and (2), if Assumption 3.1 holds, the integral terminal sliding mode surface is defined as (13) and the attitude tracking controller (18) applies, then it obtains the following conclusions:*

- (i) *The sliding mode surface σ can converge to the origin in finite time and S can converge to a small region around the origin in finite time;*
- (ii) *\tilde{q} and $\tilde{\omega}$ can converge into small regions around the expected equilibrium in finite time.*

Proof: The candidate Lyapunov function is defined as

$$V_1 = \frac{1}{2} \sigma^T J_0 \sigma \tag{19}$$

Taking the derivative of V_1 and substituting controller (18) yields

$$\begin{aligned} \dot{V}_1 &= \sigma^T \left(\dot{\delta} - l \operatorname{sgn}(\sigma) \right) \leq \|\sigma\|_1 \left(\|\dot{\delta}\|_1 - l \right) \leq -\varepsilon_0 \|\sigma\|_2 \\ &\leq -\frac{\sqrt{2}\varepsilon_0}{\sqrt{\lambda_{\max}(J_0)}} \cdot \left(\frac{1}{2} \sigma^T J_0 \sigma \right)^{\frac{1}{2}} \end{aligned} \tag{20}$$

where $\lambda_{\max}(J_0)$ is the maximum eigenvalue of J_0 and $\varepsilon_0 = l - \|\dot{\delta}\|_1$ is a positive constant. Then it yields

$$\dot{V}_1 \leq -\mu_0 V_1^{\frac{1}{2}} \tag{21}$$

where $\mu_0 = \sqrt{2}\varepsilon_0 / \sqrt{\lambda_{\max}(J_0)}$ is a positive constant. Using Lemma 3.2, $\sigma = 0$ can be reached in finite time. Then it obtains $\dot{S} = -k_1 S - k_2 \beta(S)$. Define the candidate Lyapunov function as $V_2 = \frac{1}{2} S^T S$, taking the derivative of which yields

$$\dot{V}_2 = S^T (-k_1 S - k_2 \beta(S)) \tag{22}$$

For $|S_i| > \eta_1$, it yields

$$\dot{V}_2 \leq -2\alpha_1 V_2 - 2^{\frac{\gamma_1+1}{2}} \alpha_2 V_2^{\frac{\gamma_1+1}{2}} \tag{23}$$

Based on Lemma 3.3, $|S_i| \leq \eta_1$ could be reached in finite time. Then (22) becomes

$$\begin{aligned} \dot{V}_2 &= -\frac{1}{2} (\alpha_1 + \alpha_2 r) \cdot (2S^T S) - \alpha_2 r_2 \sum_{i=1}^3 (|S_i| \cdot S_i^2) \\ &\leq -\frac{1}{2} (\alpha_1 + \alpha_2 r) \cdot V_2 \end{aligned} \tag{24}$$

S could converge to the origin asymptotically and into a small region around the origin in finite time which can be expressed as $|S_i| \leq \phi_i$ where ϕ_i can converge to the origin as time tends to infinity.

Now (i) has been proved.

Proof of (ii): When $|\tilde{q}_i| > \eta$ for $i = 1, 2, 3$, it obtains

$$\tilde{\omega}_i + \alpha_1 \tilde{q}_i + \alpha_2 \operatorname{sgn}(\tilde{q}_i) |\tilde{q}_i|^\gamma = S_i \tag{25}$$

which can be rewritten as:

$$\tilde{\omega}_i + \left(\alpha_1 - \frac{S_i}{\tilde{q}_i} \right) \tilde{q}_i + \alpha_2 \operatorname{sgn}(\tilde{q}_i) |\tilde{q}_i|^\gamma = 0 \tag{26}$$

$$\tilde{\omega}_i + \alpha_1 \tilde{q}_i + \left(\alpha_2 - \frac{S_i}{\operatorname{sgn}(\tilde{q}_i) |\tilde{q}_i|^\gamma} \right) \operatorname{sgn}(\tilde{q}_i) |\tilde{q}_i|^\gamma = 0 \tag{27}$$

As long as $\alpha_1 > |S_i|/|\tilde{q}_i|$ or $\alpha_2 > |S_i|/|\tilde{q}_i|^\gamma$ are satisfied, (26) or (27) become a classical FTSM and fast finite-time convergence for \tilde{q}_i and $\tilde{\omega}_i$ can be assured, until $|\tilde{q}_i| \leq |S_i|/\alpha_1$ and $|\tilde{q}_i|^\gamma \leq |S_i|/\alpha_2$ have all been reached. Using $|S_i| \leq \phi_i$ and $|\tilde{q}_i| > \eta$, the following regions can be reached in finite time:

$$|\tilde{q}_i| \leq Q_i \triangleq \max \left\{ \eta, \min \left\{ \frac{|\phi_i|}{\alpha_1}, \left| \frac{\phi_i}{\alpha_2} \right|^{\frac{1}{\gamma}} \right\} \right\} \tag{28}$$

$$|\tilde{\omega}_i| \leq |S_i| + \alpha_1 |\tilde{q}_i| + \alpha_2 |\tilde{q}_i|^\gamma \leq \phi_i + \alpha_1 Q_i + \alpha_2 Q_i^\gamma \tag{29}$$

Now (ii) has been proved.

The proof of Theorem 3.1 is completed.

Remark 3.2. Since \dot{S} in (13) is not available, it will be impossible to use the information of σ directly to formulate the feedback control law (18). In [13], an alternative way is proposed to get the information of $\text{sgn}(\sigma)$, which involves defining a function as:

$$g(t) = \int_0^t \sigma dt = S + \int_0^t (k_1 S + k_2 \beta(S)) dt \tag{30}$$

Therefore, $\text{sgn}(\sigma)$ can be approximately calculated as:

$$\text{sgn}(\sigma) = \text{sgn}(g(t) - g(t - \tau)) \tag{31}$$

where τ is a time delay. Since $\sigma(t) = \lim_{\tau \rightarrow 0} (g(t) - g(t - \tau))/\tau$, it gets the approximation of $\text{sgn}(\sigma)$.

3.2. Adaptive integral terminal sliding mode controller design. To deal with unknown system uncertainty and provide chattering-free finite-time control efforts at the same time, the adaptive control method is introduced to combine with the ITSMS in this subsection. A second-order differentiator [22,23] is firstly designed to achieve the approximation of \dot{S} :

$$\begin{aligned} \dot{z}_0 &= v_0 \\ v_0 &= -\lambda_1 |z_0 - S|^{\frac{2}{3}} \text{sgn}(z_0 - S) + z_1 \\ \dot{z}_1 &= v_1 \\ v_1 &= -\lambda_2 |z_1 - v_0|^{\frac{2}{3}} \text{sgn}(z_1 - v_0) + z_2 \\ \dot{z}_2 &= -\lambda_3 \text{sgn}(z_2 - v_1) \end{aligned} \tag{32}$$

where S is defined in (7), z_0 , z_1 and z_2 are estimates of S , \dot{S} and \ddot{S} respectively.

A new sliding mode surface $\hat{\sigma}$ based on the approximation of \dot{S} is then defined as:

$$\hat{\sigma} = z_1 + k_1 S + k_2 \beta(S) \tag{33}$$

where k_1 , k_2 and $\beta(\cdot)$ are the same as (13). Denote $e_1 = \dot{S} - z_1$ as the estimation error of \dot{S} . Referring to [22], e_1 will reach zero in finite time. (33) can be rewritten as:

$$\begin{aligned} \hat{\sigma} &= \dot{S} + k_1 S + k_2 \beta(S) - e_1 \\ &= J_0^{-1} F + J_0^{-1} u + \alpha_1 \dot{q}_v + \alpha_2 \dot{\beta}(\tilde{q}_v) + J_0^{-1} \delta - e_1 + k_1 S + k_2 \beta(S) \end{aligned} \tag{34}$$

Denote $\delta^* = J_0^{-1} \delta - e_1$ as the new total uncertainty which contains modeling uncertainty, external disturbance and estimation error e_1 . Inspired by the works of [13,24], an adaptive chattering-free finite-time controller is proposed as:

$$u = -F - \alpha_1 J_0 \dot{q}_v - \alpha_2 J_0 \dot{\beta}(\tilde{q}_v) - k_1 J_0 S - k_2 J_0 \beta(S) + u_1 \tag{35}$$

$$\dot{u}_1 + \lambda u_1 = u_a + u_n \tag{36}$$

$$u_a = \begin{cases} 0, & \text{if } \hat{\sigma} = 0 \\ -\frac{\hat{\sigma}}{\|\hat{\sigma}\|_2} (\hat{c}_0 + \hat{c}_1 \|\tilde{\omega}\|_2 + \hat{c}_2 \|\tilde{\omega}\|_2^2 + \hat{c}_3 \|\tilde{\omega}\|_2^3), & \text{if } \hat{\sigma} \neq 0 \end{cases} \tag{37}$$

$$u_n = \begin{cases} 0, & \text{if } \hat{\sigma} = 0 \\ -\frac{\hat{\sigma}}{\|\hat{\sigma}\|_2} k_0, & \text{if } \hat{\sigma} \neq 0 \end{cases} \tag{38}$$

$$\dot{\hat{c}}_n = p_n (\|\hat{\sigma}\|_2 \|\tilde{\omega}\|_2^n - \chi_n \hat{c}_n), \quad n = 0, 1, 2, 3 \tag{39}$$

where λ , k_0 , p_0 , p_1 , p_2 , p_3 , χ_0 , χ_1 , χ_2 and χ_3 are all positive control parameters. \hat{c}_0 , \hat{c}_1 , \hat{c}_2 and \hat{c}_3 are the adaptive parameters. The derivative of $\hat{\sigma}$ is $\dot{\hat{\sigma}} = \dot{\delta}^* - \lambda u_1 + u_a + u_n$. To facilitate controller (35), the following assumption is introduced.

Assumption 3.2. [9,24] $\dot{\delta}^* - \lambda u_1$ is assumed to be bounded and can be expressed as

$$\left\| \dot{\delta}^* - \lambda u_1 \right\|_2 \leq c_1 + c_2 \|\tilde{\omega}\|_2 + c_3 \|\tilde{\omega}\|_2^2 + c_4 \|\tilde{\omega}\|_2^3 \quad (40)$$

where c_1, c_2, c_3 and c_4 are unknown positive constants and will be adjusted on line by the adaptive laws defined as (39).

Remark 3.3. For Assumption 2 in [24], the lumped term T_d of the disturbances and modeling uncertainties satisfies $\|T_d\| \leq \gamma_0(1 + \|\omega\| + \|\omega\|^2)$ where γ_0 is an unknown positive constant and ω is the angular velocity tracking error defined by [24]. The highest power of $\|\omega\|$ that occurs in \dot{T}_d is $\|\omega\|^3$. Then it yields $\|\dot{T}_d\| \leq c_0 + c_1 \|\omega\| + c_2 \|\omega\|^2 + c_3 \|\omega\|^3$, where c_0, c_1, c_2 and c_3 are positive constants. Then it obtains Assumption 3.2.

Theorem 3.2. Consider systems (1) and (2), if Assumption 3.2 holds the second-order differentiator is defined as (32), the integral terminal sliding mode surface is defined as (13) and the attitude tracking controller is designed as (35), then it obtains the following conclusions:

- (i) σ and S can converge into small regions around the origin in finite time;
- (ii) \tilde{q} and $\tilde{\omega}$ can converge into small regions around the expected equilibrium in finite time.

Proof: The Lyapunov function candidate is selected as

$$V_3 = \frac{1}{2} \hat{\sigma}^T J_0 \hat{\sigma} + \frac{1}{2} \sum_{n=0}^3 \frac{1}{p_n} \tilde{c}_n^2 \quad (41)$$

where $\tilde{c}_n = c_n - \hat{c}_n$ for $n = 0, 1, 2, 3$ are the estimation errors.

Taking the derivative of V_3 and substituting (35) obtains

$$\begin{aligned} \dot{V}_3 &= \hat{\sigma}^T \left(\dot{\delta}^* - \lambda u_1 + u_a + u_n \right) - \sum_{n=0}^3 \frac{1}{p_n} \tilde{c}_n \dot{\hat{c}}_n \\ &\leq \|\hat{\sigma}\|_2 \left\| \dot{\delta}^* - \lambda u_1 \right\|_2 - (\hat{c}_0 + \hat{c}_1 \|\tilde{\omega}\|_2 + \hat{c}_2 \|\tilde{\omega}\|_2^2 + \hat{c}_3 \|\tilde{\omega}\|_2^3) \|\hat{\sigma}\|_2 \\ &\quad - k_0 \|\hat{\sigma}\|_2 - \sum_{n=0}^3 \frac{1}{p_n} \tilde{c}_n \dot{\hat{c}}_n \\ &= (c_0 + c_1 \|\tilde{\omega}\|_2 + c_2 \|\tilde{\omega}\|_2^2 + c_3 \|\tilde{\omega}\|_2^3) \|\hat{\sigma}\|_2 \\ &\quad - (\hat{c}_0 + \hat{c}_1 \|\tilde{\omega}\|_2 + \hat{c}_2 \|\tilde{\omega}\|_2^2 + \hat{c}_3 \|\tilde{\omega}\|_2^3) \|\hat{\sigma}\|_2 - k_0 \|\hat{\sigma}\|_2 - \sum_{n=0}^3 \frac{1}{p_n} \tilde{c}_n \dot{\hat{c}}_n \\ &\leq -k_0 \|\hat{\sigma}\|_2 - \sum_{n=0}^3 \chi_n (\hat{c}_n - c_n) \hat{c}_n \end{aligned} \quad (42)$$

Using the inequalities of $-(\hat{c}_n - c_n) \hat{c}_n \leq -(\hat{c}_n - \frac{1}{2}c_n)^2 + \frac{1}{2}c_n^2$ ($n = 0, 1, 2, 3$), (42) becomes

$$\begin{aligned} \dot{V}_3 &\leq -k_0 \|\hat{\sigma}\|_2 - \sum_{n=0}^3 \chi_n \left(\hat{c}_n - \frac{c_n}{2} \right)^2 + \sum_{n=0}^3 \chi_n \cdot \frac{c_n^2}{2} \\ &\leq -k_0 \|\hat{\sigma}\|_2 - \sum_{n=0}^3 \chi_n |\hat{c}_n - c_n| + \sum_{n=0}^3 \left(\frac{\chi_n c_n^2}{2} + \chi_n |\hat{c}_n - c_n| \right) \\ &\leq -k_0 \|\hat{\sigma}\|_2 - \sum_{n=0}^3 \chi_n |\hat{c}_n - c_n| + \sum_{n=0}^3 \left(\frac{\chi_n c_n^2}{2} + \chi_n |c_n| \right) \end{aligned} \quad (43)$$

Based on Lemma 3.1, it obtains

$$\dot{V}_3 \leq -\alpha \left[\left(\frac{1}{2} \hat{\sigma}^T J_0 \hat{\sigma} \right)^{0.5} + \sum_{n=0}^3 \left(\frac{\tilde{c}_n^2}{2p_n} \right)^{0.5} \right] + \chi \leq -\alpha V_3^{0.5} + \chi \quad (44)$$

where both $\alpha = \min \left(\sqrt{2}k_0 / \sqrt{\lambda_{\max}(J_0)}, \chi_0 \sqrt{2p_0}, \chi_1 \sqrt{2p_1}, \chi_2 \sqrt{2p_2}, \chi_3 \sqrt{2p_3} \right)$ and $\chi = \sum_{n=0}^3 \left(\frac{1}{2} \chi_n c_n^2 + \chi_n |c_n| \right)$ can be adjusted by the controllers parameters (44) can be rewritten as

$$\dot{V}_3 \leq - \left(\alpha - \frac{\chi}{V_3^{0.5}} \right) V_3^{0.5} \quad (45)$$

Based on Lemma 3.2, as long as $\alpha - \chi/V_3^{0.5} > 0$ is satisfied, the convergence of (45) is assured. The time consumption T_1 for $V_3^{0.5} \leq \chi/\alpha$ to be reached can be estimated as $T_1 \leq 2V_3^{0.5}(0)/(\alpha - \chi/V_3^{0.5}(t))$ which may tend to infinity as $\alpha - \chi/V_3^{0.5}(t)$ tends to 0.

Considering the definition of V_3 in (41), it yields

$$V_3^{0.5} \geq \left(\frac{1}{2} \hat{\sigma}^T J_0 \hat{\sigma} \right)^{0.5} \geq \sqrt{\frac{\lambda_{\min}(J_0)}{2}} \|\hat{\sigma}\|_2 \quad (46)$$

where $\lambda_{\min}(J_0)$ is the minimum eigenvalue of J_0 . Using $V_3^{0.5} \leq \chi/\alpha$ and (46) yields $|\hat{\sigma}_i| \leq \chi/\alpha \sqrt{2/\lambda_{\min}(J_0)}$. As a result, though $|\hat{\sigma}_i| \leq \chi/\alpha \sqrt{2/\lambda_{\min}(J_0)}$ may be reached as time tends to infinity, the convergence of $\hat{\sigma}$ toward $\chi/\alpha \sqrt{2/\lambda_{\min}(J_0)}$ can still be achieved which can be expressed as $|\hat{\sigma}_i| \leq \kappa_i$ ($i = 1, 2, 3$) and the limit of κ_i is $\chi/\alpha \sqrt{2/\lambda_{\min}(J_0)}$ with time going to infinity. Given the finite-time convergence property of (32), $|\sigma_i| \leq \kappa_i$ ($i = 1, 2, 3$) can also be reached in finite time.

To analyze the dynamic characteristic of S , the following Lyapunov candidate function is defined:

$$V_4 = \frac{1}{2} S^T S \quad (47)$$

Taking the derivative of V_4 , substituting (13) and considering $|S_i| > \eta_1$ yields

$$\dot{V}_4 = S^T (-k_1 S - k_2 \text{sig}^{\gamma_1}(S) + \sigma) \quad (48)$$

which can be further rearranged into the following two forms for $i = 1, 2, 3$:

$$\dot{V}_4 = -S^T \left[\text{diag} \left(k_1 - \frac{\sigma_i}{S_i} \right) S + k_2 \text{sig}^{\gamma_1}(S) \right] \quad (49)$$

$$\dot{V}_4 = -S^T \left[k_1 S + \text{diag} \left(k_2 - \frac{\sigma_i}{\text{sgn}(S_i) |S_i|^{\gamma_1}} \right) \text{sig}^{\gamma_1}(S) \right] \quad (50)$$

where $\text{diag}(x_i)$ represents a diagonal matrix with diagonal elements of x_i , $i = 1, 2, 3$.

If $k_1 > |\sigma_i|/|S_i|$ or $k_2 > |\sigma_i|/|S_i|^{\gamma_1}$ for $i = 1, 2, 3$ are satisfied, the matrixes of $\text{diag}(k_1 - \sigma_i/S_i)$ or $\text{diag}(k_2 - \sigma_i/\text{sgn}(S_i) |S_i|^{\gamma_1})$ can be kept positive, which yields $\dot{V}_4 \leq -(2k_2/\lambda_{\max}(J_0))^{(\gamma_1+1)/2} \left(\frac{1}{2} S^T J_0 S \right)^{(\gamma_1+1)/2}$ and $\dot{V}_4 \leq -(2k_1/\lambda_{\max}(J_0)) \left(\frac{1}{2} S^T J_0 S \right)$ where $\lambda_{\max}(J_0)$ is the maximum eigenvalue of J_0 . Based on Lemma 3.2 and Lyapunov stability theory, convergence of the closed-loop system is obtained until $k_1 \leq |\sigma_i|/|S_i|$ and $k_2 \leq |\sigma_i|/|S_i|^{\gamma_1}$ have all been reached. As a result, S can converge into the following regions in finite time:

$$|S_i| \leq \varphi_i \triangleq \min \left\{ \frac{|\kappa_i|}{k_1}, \left| \frac{\kappa_i}{k_2} \right|^{\frac{1}{\gamma_1}} \right\}, \quad i = 1, 2, 3 \quad (51)$$

where κ_i is the upper bound of σ_i ($i = 1, 2, 3$).

The stability analysis for \tilde{q}_v and $\tilde{\omega}$ is similar to the proof of (ii) within Theorem 3.1 and can be omitted here. The following results can be obtained:

$$|\tilde{q}_i| \leq Q_i \triangleq \max \left\{ \eta, \min \left\{ \frac{|\varphi_i|}{\alpha_1}, \left| \frac{\varphi_i}{\alpha_2} \right|^{\frac{1}{\gamma}} \right\} \right\} \quad (52)$$

$$|\tilde{\omega}_i| \leq |S_i| + \alpha_1 |\tilde{q}_i| + \alpha_2 |\tilde{q}_i|^\gamma \leq \varphi_i + \alpha_1 Q_i + \alpha_2 Q_i^\gamma \quad (53)$$

where φ_i ($i = 1, 2, 3$) is defined in (51).

Now (i) and (ii) have been proved. The proof of Theorem 3.2 is completed.

4. Numerical Examples. To illustrate the effectiveness of the proposed control methods, numerical simulations are conducted. Based on the works of [11,18], initial values of the spacecraft system are decided. The nominal inertia matrix J_0 , initial quaternion $q(0)$, initial angular velocity $\omega(0)$, inertia uncertainty ΔJ , external disturbance d and desired angular velocity ω_d are designed as:

$$J_0 = [20, 1.2, 0.9; 1.2, 17, 1.4; 0.9, 1.4, 15] \text{ kg}\cdot\text{m}^2$$

$$q(0) = [0.4031, -0.2584, 0.7386, 0.4745]^T$$

$$\omega(0) = [0, 0, 0]^T \text{ rad/s}$$

$$\Delta J = \text{diag}\{\sin(0.1t), 2 \sin(0.2t), 3 \sin(0.3t)\} \text{ kg}\cdot\text{m}^2$$

$$d = 0.1 \times [\sin(0.1t), 2 \cos(0.2t), 3 \sin(0.3t)]^T \text{ N}\cdot\text{m}$$

$$\omega_d = [0.1 \sin(t/40), -0.1 \sin(t/50), -0.1 \sin(t/60)]^T \text{ rad/s}$$

Parameters for the second-order differentiator defined in (32) are set as: $\lambda_1 = 2$, $\lambda_2 = 0.8$ and $\lambda_3 = 0.3$. The simulation time is set as 100 seconds. 3 different groups of simulations are undertaken under the same initial values defined above.

The first group is under controller (18), parameters of which are set as: $\eta = 0.001$, $\eta_1 = 0.001$, $\gamma = 0.9$, $\alpha_1 = 0.5$, $\alpha_2 = 1.8$, $\gamma_1 = 0.5$, $k_1 = 0.05$, $k_2 = 0.4$ and $l = 0.2$. The simulation results are presented in Figures 1-3. As shown in Figures 1 and 2, \tilde{q} and $\tilde{\omega}$ can be stabilized within less than 10 seconds with accuracy of 3×10^{-6} and 4×10^{-5} ,

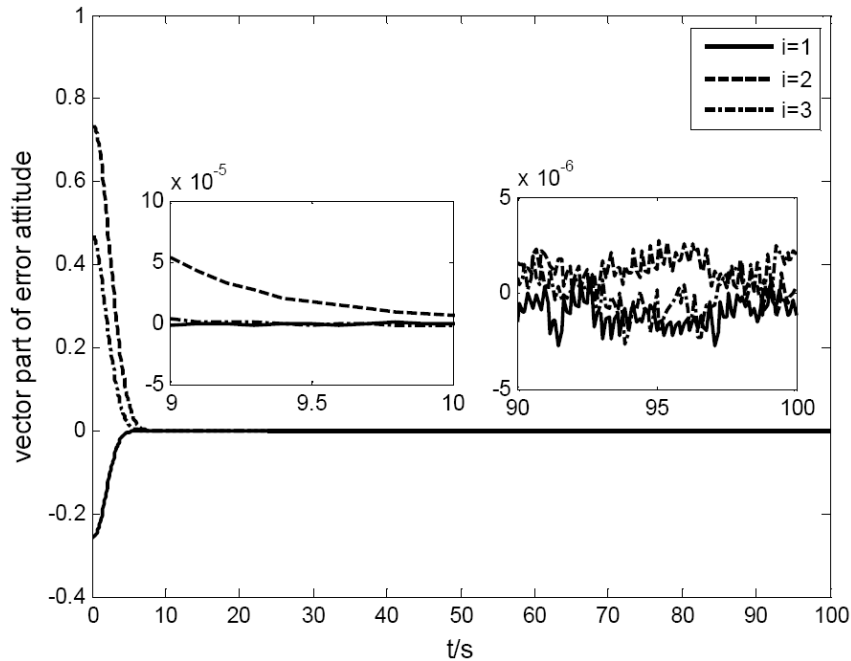


FIGURE 1. The curves of \tilde{q}_v under (18)

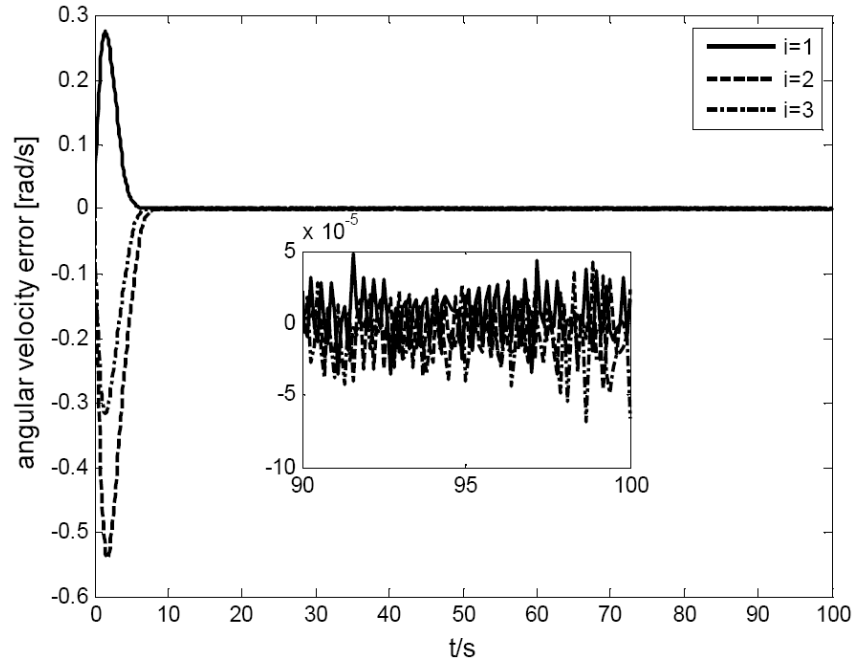
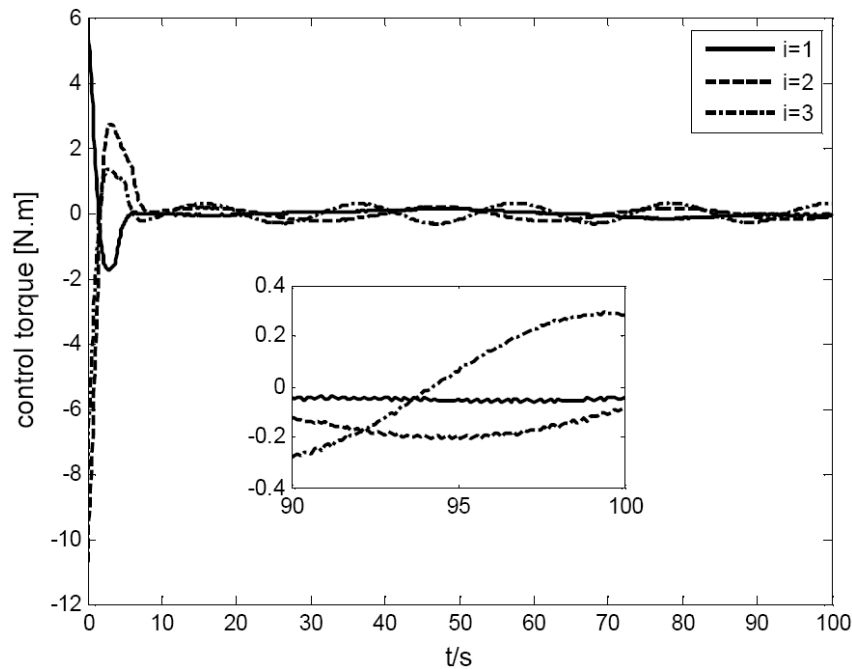
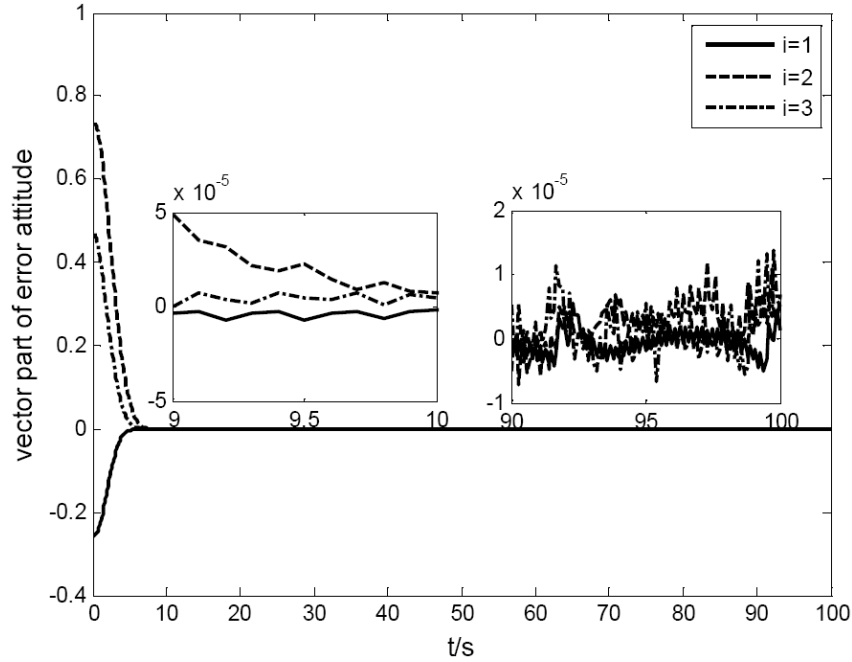
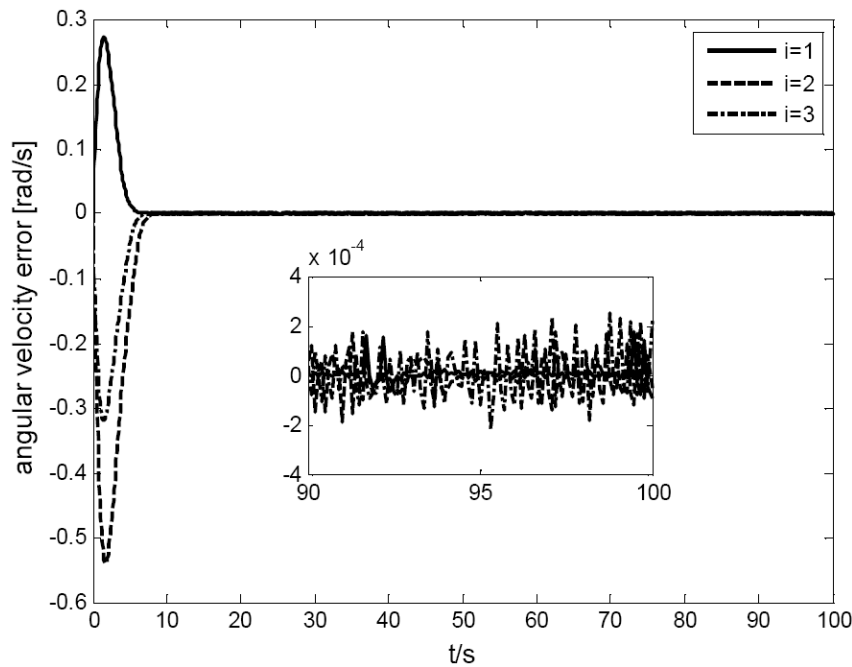
FIGURE 2. The curves of $\tilde{\omega}$ under (18)

FIGURE 3. The curves of control torque of controller (18)

respectively. Figure 3 shows the actual control torques can be constrained to ± 0.4 N·m at last.

The second group is under controller (18), parameters of which are set as: $\eta = 0.001$, $\eta_1 = 0.001$, $\gamma = 0.9$, $\alpha_1 = 0.5$, $\alpha_2 = 1.8$, $\gamma_1 = 0.5$, $k_1 = 0.05$, $k_2 = 0.4$ and $l = 2$. The simulation results are presented in Figures 4-6. As shown in Figures 4 and 5, \tilde{q} and $\tilde{\omega}$ can be stabilized within less than 10 seconds with accuracy of 3×10^{-6} and 4×10^{-5} , respectively. Figure 6 shows the control torques can be constrained to ± 0.4 N·m at last.

FIGURE 4. The curves of \tilde{q}_v under (18)FIGURE 5. The curves of $\tilde{\omega}$ under (18)

The third group is under controller (35), parameters of which are set as: $\eta = \eta_1 = 0.001$, $\gamma = 0.9$, $\alpha_1 = 0.5$, $\alpha_2 = 1.8$, $\gamma_1 = 0.5$, $k_1 = 0.05$, $k_2 = 0.4$, $\lambda = 1$, $k_0 = 0.001$, $p_0 = p_1 = p_2 = p_3 = 1$ and $\chi_0 = \chi_1 = \chi_2 = \chi_3 = 1$. The simulation results are presented in Figures 7-10. It can be seen from Figures 7 and 8, \tilde{q} and $\tilde{\omega}$ can also be stabilized in 10 seconds with accuracy of 6×10^{-4} and 4×10^{-4} , respectively. Figure 9 illustrates that the control torques can be constrained to ± 0.4 N·m at last. Figure 10 shows that at last the adaptive parameters are bounded by 0.03.

Through comparison of the simulation results, it can be observed that:

(1) As seen from Figure 3, Figure 6 and Figure 10, the proposed controllers in this paper are chattering-free, which agrees with the analysis of Theorem 3.1 and Theorem 3.2 and verifies the advantages of the proposed controllers compared with the switch controller in [10].

(2) Comparison of group 1 and group 2 shows that, parameter l with larger values may lead to control precision decrease and more serious fluctuation. However, since the sign functions within (18) and (35) are all hidden behind the integration operation, the resultant control laws are still continuous and without chattering phenomenon.

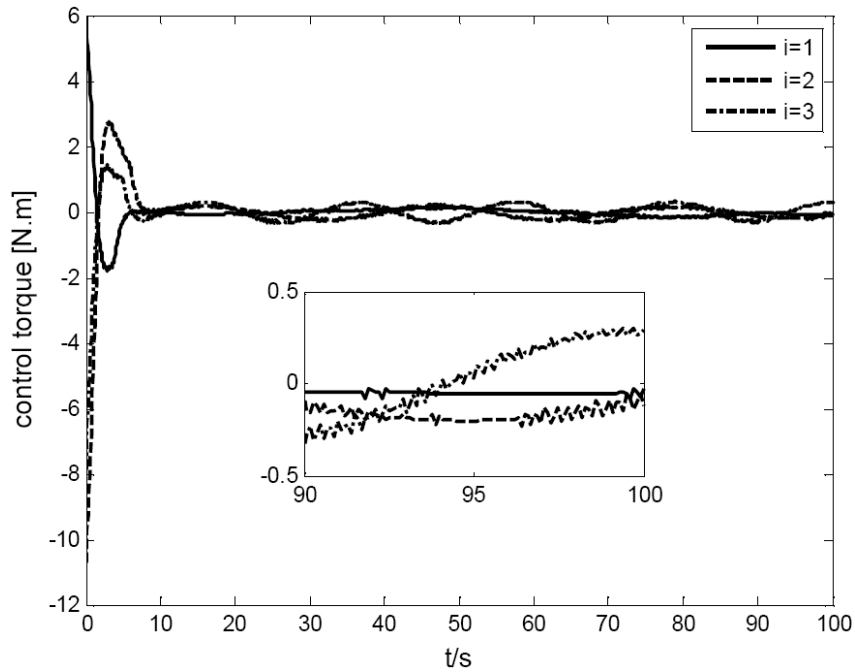


FIGURE 6. The curves of control torque of controller (18)

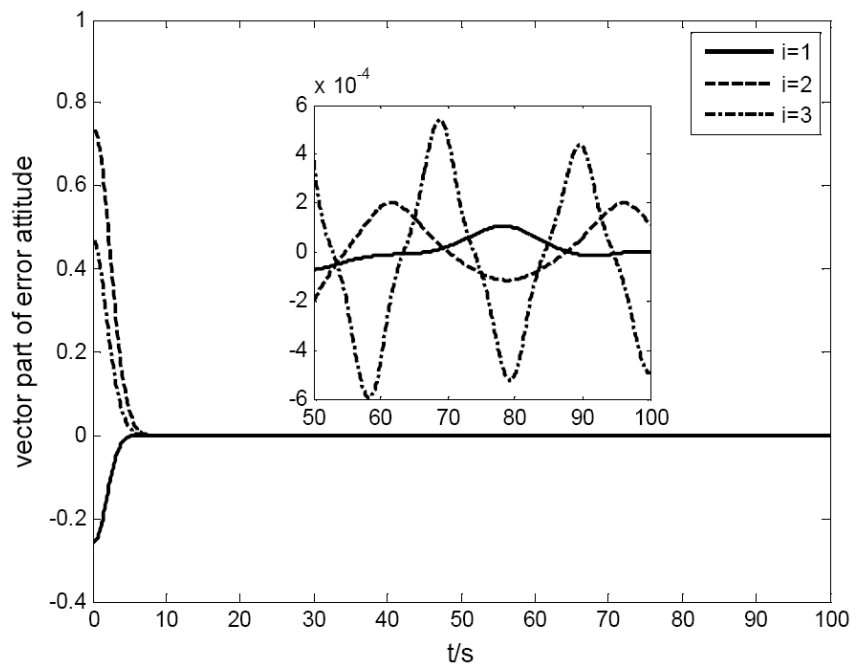


FIGURE 7. The curves of \tilde{q}_v under (35)

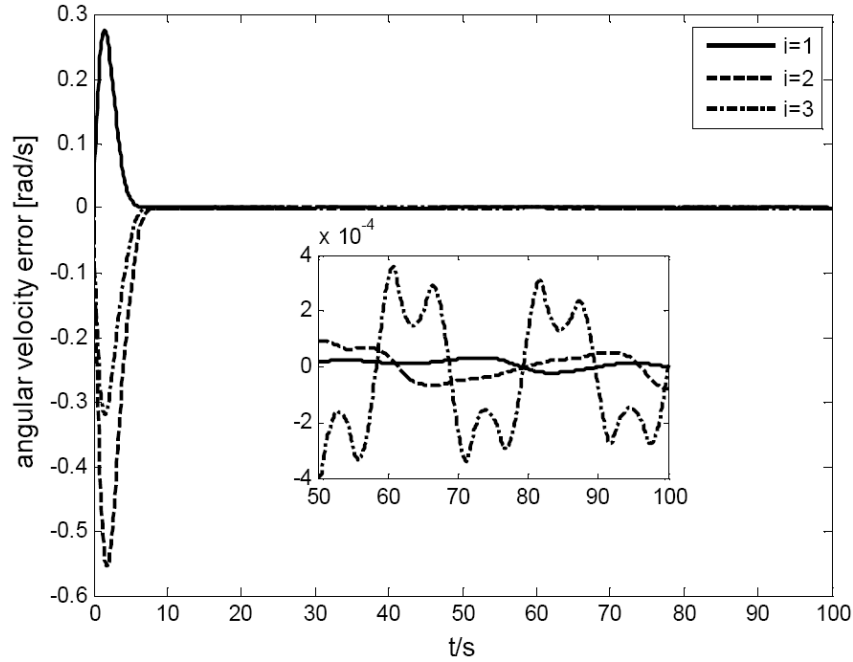
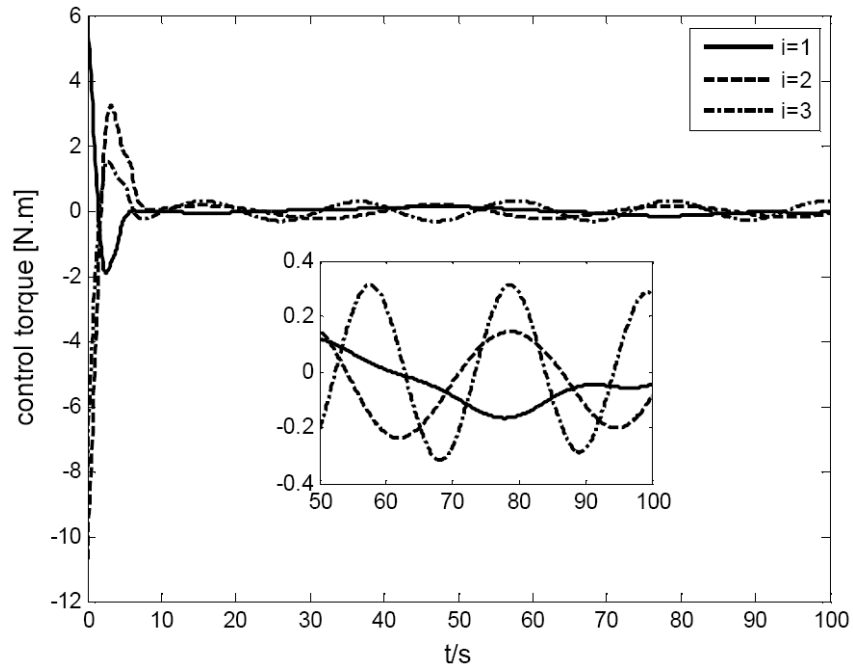
FIGURE 8. The curves of $\tilde{\omega}$ under (35)

FIGURE 9. The curves of control torque of controller (35)

(3) The attitude tracking control missions can all be finished in finite time with satisfactory control accuracy. Controller (18) in group 1 achieves higher control precisions, since theoretically under (18) the tracking errors can reach the expected equilibriums, but controller (35) only assures ultimate boundedness for the system. However, in controller (18) l must be large enough and decided using priori information of system uncertainty which restricts the application scope of this method. While for controller (35), with the help of the adaptive control procedure, parameters \hat{c}_n ($n = 0, 1, 2, 3$) can be adjusted on line and have much smaller values, which obtains more smooth simulation results.

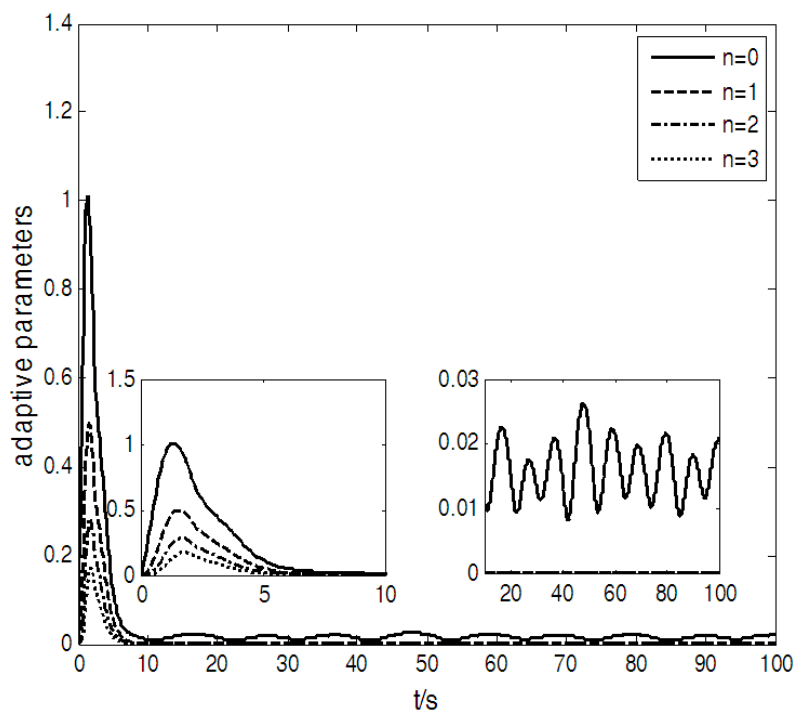


FIGURE 10. The curves of adaptive parameters under (35)

5. Conclusions. This paper researches the attitude tracking problem of rigid spacecraft under inertia uncertainty and external disturbance with two different controllers designed. Benefits of the proposed two controllers include finite time convergence, chattering-free control input and robustness against system uncertainty. Stability of the closed-loop system has been proved through Lyapunov stability theory. Simulations are undertaken to show the effectiveness of the controllers.

Acknowledgment. The authors would like to acknowledge the financial support provided by the National Natural Science Foundation of China under Grant 61174037 and the State Key Program of National Natural Science of China under Grant NSFC-61333003.

REFERENCES

- [1] W. Luo, Y. C. Chu and K. V. Ling, Inverse optimal adaptive control for attitude tracking of spacecraft, *IEEE Trans. Automatic Control*, vol.50, no.11, pp.1639-1654, 2005.
- [2] B. Zhang and S. Song, Robust attitude coordination control of formation flying spacecraft under control input saturation, *International Journal of Innovative Computing, Information and Control*, vol.7, no.7, pp.1060-1069, 2011.
- [3] R. Kristiansen, P. J. Nicklasson and J. T. Gravdahl, Satellite attitude control by quaternion-based backstepping, *IEEE Trans. Control Systems Technology*, vol.17, no.1, pp.227-232, 2009.
- [4] J. Ahmed, V. T. Coppola and D. S. Bernstein, Asymptotic tracking of spacecraft attitude motion with inertia matrix identification, *Journal of Guidance Control & Dynamics*, vol.21, no.5, pp.684-691, 1998.
- [5] H. Xing, D. Li and X. Zhong, Sliding mode control for a class of parabolic uncertain distributed parameter systems with time-varying delays, *International Journal of Innovative Computing, Information and Control*, vol.5, no.9, pp.2689-2702, 2009.
- [6] K. D. Young, V. I. Utkin and U. Ozguner, A control engineer's guide to sliding mode control, *IEEE Trans. Control Systems Technology*, vol.7, no.3, pp.328-342, 1999.
- [7] V. I. Utkin, Sliding mode control design principles and applications to electric drives, *IEEE Trans. Industrial Electronics*, vol.40, no.1, pp.23-36, 1993.
- [8] Y. Tang, Terminal sliding mode control for rigid robots, *Automatica*, vol.34, no.1, pp.51-56, 1998.

- [9] K. Lu and Y. Xia, Finite-time fault-tolerant control for rigid spacecraft with actuator saturations, *IET Control Theory & Applications*, vol.7, no.11, pp.1529-1539, 2013.
- [10] S. Wu, G. Radice, Y. Gao and Z. Sun, Quaternion-based finite time control for spacecraft attitude tracking, *Acta Astronautica*, vol.69, nos.1-2, pp.48-58, 2011.
- [11] K. Lu and Y. Xia, Adaptive attitude tracking control for rigid spacecraft with finite-time convergence, *Automatica*, vol.49, no.12, pp.3591-3599, 2013.
- [12] E. Jin and Z. Sun, Robust controllers design with finite time convergence for rigid spacecraft attitude tracking control, *Aerospace Science & Technology*, vol.12, no.4, pp.324-330, 2008.
- [13] Y. Feng, F. Han and X. Yu, Chattering free full-order sliding-mode control, *Automatica*, vol.50, no.4, pp.1310-1314, 2014.
- [14] Z. Zhu, Y. Xi and M. Fu, Attitude stabilization of rigid spacecraft with finite-time convergence, *International Journal of Robust & Nonlinear Control*, vol.21, no.6, pp.686-702, 2011.
- [15] A. M. Zou, K. D. Kumar, Z. G. Hou and X. Liu, Finite-time attitude tracking control for spacecraft using terminal sliding mode and Chebyshev neural network, *IEEE Trans. Systems Man & Cybernetics, Part B: Cybernetics*, vol.41, no.4, pp.950-963, 2011.
- [16] L. Wang, T. Chai and L. Zhai, Neural-network-based terminal sliding-mode control of robotic manipulators including actuator dynamics, *IEEE Trans. Industrial Electronics*, vol.56, no.9, pp.3296-3304, 2009.
- [17] Q. Hu, B. Li and J. Qi, Disturbance observer based finite-time attitude control for rigid spacecraft under input saturation, *Aerospace Science & Technology*, vol.39, pp.13-21, 2014.
- [18] C. Pukdeboon and P. Siricharuanun, Nonsingular terminal sliding mode based finite-time control for spacecraft attitude tracking, *International Journal of Control Automation & Systems*, vol.12, no.3, pp.530-540, 2014.
- [19] K. Lu, Y. Xia and M. Fu, Controller design for rigid spacecraft attitude tracking with actuator saturation, *Information Sciences*, vol.220, no.220, pp.343-366, 2013.
- [20] S. Yu, X. Yu, B. Shirinzadeh and Z. Man, Continuous finite time control for robotic manipulators with terminal sliding mode, *Automatica*, vol.41, no.11, pp.1957-1964, 2005.
- [21] M. Eom and D. Chwa, Adaptive integral sliding mode control for nuclear research reactor with system uncertainties and input perturbation, *Electronics Letters*, vol.52, no.4, pp.272-274, 2016.
- [22] C. Pukdeboon, Adaptive backstepping finite-time sliding mode control of spacecraft attitude tracking, *Journal of Systems Engineering & Electronics*, no.4, pp.826-839, 2015.
- [23] K. P. Ramesh, A. Chalanga and B. Bandyopadhyay, Smooth integral sliding mode controller for the position control of Stewart platform, *ISA Transactions*, vol.58, pp.543-551, 2015.
- [24] Q. Shen, D. Wang, S. Zhu and E. K. Poh, Finite-time fault-tolerant attitude stabilization for spacecraft with actuator saturation, *IEEE Trans. Aerospace & Electronic Systems*, vol.51, no.3, pp.2390-2405, 2015.